

Evaluation of 3-dimensional Electrical Impedance Tomography-Arrays for Underwater Object Detection

Sven Ole Schmidt, Fabian John and Horst Hellbrück
Technische Hochschule Lübeck - University of Applied Sciences, Germany
Department of Electrical Engineering and Computer Science
Email: {sven.ole.schmidt, fabian.john, horst.hellbrueck}@th-luebeck.de

Abstract—Underwater detection and localization infrastructure has gained more importance in the recent years. Buried objects like high-voltage power transmission cables need to be localized reliably. For successful localization, the detection of such objects is indispensable. The Electrical Impedance Tomography (EIT) is an imaging method, which generates an artificial current flow to detect the environment in a certain area around the EIT electrode-array. The 3-dimensional design of this array is not yet investigated for underwater detection of metallic objects. It is an open issue whether and to what extent the design influences detection. In this work, we analyze multiple EIT-array designs and evaluate their detection capability. For this, we introduce and investigate four 2- and 3-dimensional EIT-array designs. We model these designs and evaluate the measurable electrical potentials. We state, that the closer electrodes of the array are to an detectable object, the higher is the detection capability of the whole system. We also found out, that current flows in parallel to parts of the EIT-array do decrease the detection capability. In the future, we want to focus on prototyping our EIT detection system based on these results and test the detection capability in a real outdoor environment afterwards.

Index Terms—EIT, underwater object detection, detection capability, array design, COMSOL Multiphysics

I. INTRODUCTION

More and more metallic objects are found underwater or even under a sediment layer. These are, for example, unexploded ordnance (UXO) or high-voltage cables that have

a significant impact on the environment. According to German law, transmission cables must be buried at a depth of at least one meter below the sediment-water layer. This reduces the impact on flora and fauna in the vicinity. Szyrowski et al. stated that especially buried object detection, characterization, and localization for all environmental conditions with a single approach is still an unsolved challenge [1]. This increases the importance of underwater detection and localization.

The proof of existence of objects in the observation area, namely the detection, is considered in this work. The detection of metallic objects underwater is still a challenging task [2]. Over the years, a lot of research for underwater detection and localization was performed in the last years, like gradiometry methods [3], [4], [5] or ultrasonic-technologies [6], [7], [8], [9].

As long as the conductivity of the environment differs from the cable's conductivity, the detection of these objects and cables is possible. *Electrical Impedance Tomography* (EIT) is one method to detect metallic objects in an underwater environment based on the conductivity [10]. EIT is an imaging method applying on measurements of the current flow distribution. While between a pair of two emitting electrodes a current flows, the remaining measurement electrodes perceive an induced electrical potential. This potential is interfered by inhomogeneities in the conductivity, such as metallic objects. The exploitation of the conductive properties of the cable's material enables the detection of this object. In the previous work at the CoSA Center of Excellence at the Technische Hochschule Lübeck, we derived the simulative basics of EIT-systems for the detection of metallic elements in an underwater environment. We focused on the electrical permittivity of the setup [11], while now we will focus on the conductivity of the environment. These simulative assumptions are evaluable by our self-build 3D positioning system and message queue telemetry transport (MQTT) protocol based distributed underwater measurement equipment shown in [12], [13].

In this work, we take a look at the design of EIT-arrays with a focus on the underwater object detection capability. The optimal design of the electrode-array is of interest for accurate and reliable detection of metallic objects. For analysis of the EIT-array properties, we develop multiple 1-, 2- and 3-dimensional array designs. Beneath the general conception of such arrays, we model a practical implementation of each

© 2022 IEEE. Personal use of this material is permitted. Permission from IEEE must be obtained for all other uses, in any current or future media, including reprinting/republishing this material for advertising or promotional purposes, creating new collective works, for resale or redistribution to servers or lists, or reuse of any copyrighted component of this work in other works.

Cite this article: S. O. Schmidt, F. John and H. Hellbrück, "Evaluation of 3-dimensional Electrical Impedance Tomography-Arrays for Underwater Object Detection," OCEANS 2022 - Chennai, 2022, pp. 1-6, doi: 10.1109/OCEANSChennai45887.2022.9775412.

Original: <https://ieeexplore.ieee.org/abstract/document/9775412>

design case and analyzed the behavior by simulation. To create a realistic simulation environment, we perform the evaluation in an underwater scenario similar to our laboratory aquarium.

The contributions are as follows:

- We derive four self-designed 2- and 3-dimensional EIT-array designs.
- We model an EIT-system with split arrays for current emission and potential measurement
- We analyze the EIT-arrays with modeled simulations of a metallic object in a laboratory underwater environment.
- We evaluate the object detection capability of these EIT-arrays with our new metric, the distance of electrical potential d_{des} .

The rest of the paper is organized as follows. In Section II, we depict the general functionality of EIT and focus on its advantages in the field of underwater object detection. Section III introduces our concept to design the EIT electrodes in 1-,2- and 3-dimensional arrays. We will also focus on the advantages of the single designs. In Section IV, we introduce the evaluation setup and compare the single array design among themselves with respect to their detection capability. Section V concludes the paper and gives a short outlook on future work.

II. ELECTRICAL IMPEDANCE TOMOGRAPHY FOR UNDERWATER OBJECT DETECTION

Electrical Impedance Tomography (EIT) is a method to construct an image of the observation area by analyzing the measured electrical conductivity inside this area. Each EIT-array consists of multiple electrodes, as shown in Figure 1.

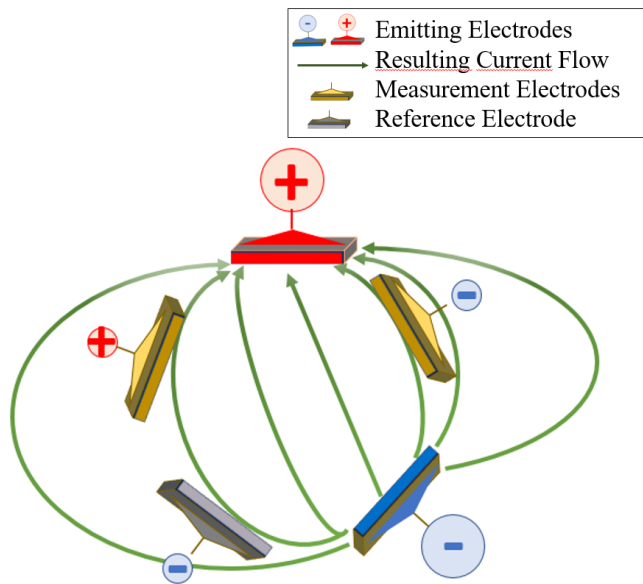


Fig. 1: General concept of EIT systems

In the following, we differ between the *emitting electrodes* and the *measurement electrodes*. A set of two emitting electrodes are provided with a variable current of a self-defined

arbitrary waveform. While one of these emitting electrodes is loaded by the current $I_1(t)$, the second electrode of the set is provided with a phase-shifted version of this current at the same time $I_2(t) = I_1(t) \cdot e^{(j \cdot 180^\circ)} = -I_1(t)$. This is needed to prevent bias current. The emitting electrodes are displayed in Figure 1 in red and blue, respectively. The measurement electrodes perceive the induced electrical potentials (in Figure 1: depicted in yellow). Additionally, we installed a *reference electrode*, which is connected to ground potential of the measurement setup (depicted in gray). To avoid reference differences of the electrical potentials of the measurement electrodes, all electrodes are grounded wrt. this reference electrode.

For complex imaging of the observation area, multiple combinations of the emitting electrodes are chosen. So successively, the electrodes which emit the current change, while the remain electrodes perceive the electrical potentials. The derivation of the conductivities is made possible by algorithms focusing on inverse problems (For further literature on this field, we recommend [14] of Kolehmainen et al.). The determination of the conductivity areas inside the observation area enables the ability of detection of metallic objects.

Since the arrangement of the EIT-array’s electrodes influence this observation area, we assume that it also influences the detection capabilities. In the upcoming section, we will focus on the design of EIT-arrays.

III. DESIGN OF THE EIT-ARRAYS

After explaining the general concept of EIT for object detection, we will now introduce the developed EIT-array designs evaluated in the subsequent Section IV.

To arrange an EIT-array, the position of the electrodes is of interest. The larger the covered area of the electrodes, the larger the observation area. But as stated in [10], with a constant number of measurement electrodes, a larger covered area decreases the resolution of the observation area’s image provided by the EIT analysis.

General design concepts for 1-, 2- and 3-dimensional EIT-arrays are shown in Figure 2.

As shown in Figure 2 Subplot (a) the 1-dimensional case only covers a line of electrodes. Although this array is easy to set up and takes up little space, measurements of the electrodes does not include information of the observation area in the y - or z - direction, since all electrodes have the same y - and z -coordinate.

The subplots of (b) depict 2-dimensional EIT-arrays. In subplot (b1) a plane of electrodes is created, while the design of subplot (b2) consists of two 1-dimensional arrays, which are perpendicular to each other. Even though two directions are covered by both designs, one direction each is not covered (subplot (b1): z not covered, subplot (b2): y not covered), since all measurement electrodes share the same respective coordinate. If the analysis of the missing direction is not of interest, this design offers a low setup due to its 2-dimensional plane.

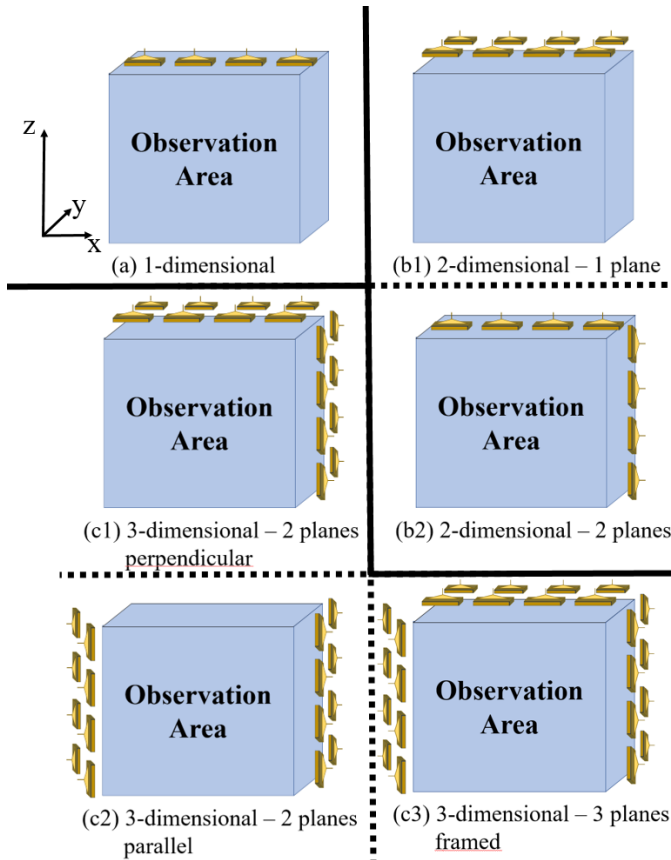


Fig. 2: Design concepts for 1-, 2- and 3-dimensional EIT-arrays.

The design of the subplots (c) introduce three 3-dimensional designs. While subplot (c1) and (c2) both include two planes of electrodes, subplot (c3) depicts a design with three planes. In (c1), the planes are installed perpendicular to each other. This design enables the measurement of electrical potentials in a certain depth defined by the planes width. In (c2), the planes are parallel to each other, which is assumed to focus on the observation area on the space between the planes, while also elements close to the plane edges are perceptible. The design of (c3) combines the previous ideas. In contrast to (c2) another plane of measurement electrodes is added, which caps the observation area in positive z -direction. Therefore the observation area is nearly framed by the electrodes. For the 3-dimensional case, all three designs contain electrodes with different positions in x -, y - and z -directions. While the set up is complex compared to the 1- and 2-dimensional case, the electrodes are able to measure the potential in all three dimensions.

For the following evaluation of the designs in Section IV, we will focus on the 2- and 3-dimensional designs (b1), (c1), (c2) and (c3).

IV. EVALUATION OF THE EIT-ARRAY DESIGNS

In this section, we will first present our evaluation setup and subsequently describe results for the single EIT-array designs.

A. Evaluation Setup

The aim of this work is to compare the object detection capability of the EIT-array designs. For evaluation, we modeled an underwater environment which is similar to our laboratory aquarium. Figure 3 depicts this environment. The modeling of the environment as well as the calculation of the electrical potentials is done with the software *COMSOL Multiphysics*. The model is based on our previous work in [11], which validated this model with an analytical approach. For the simulation environment and results, we refer to the repository¹.

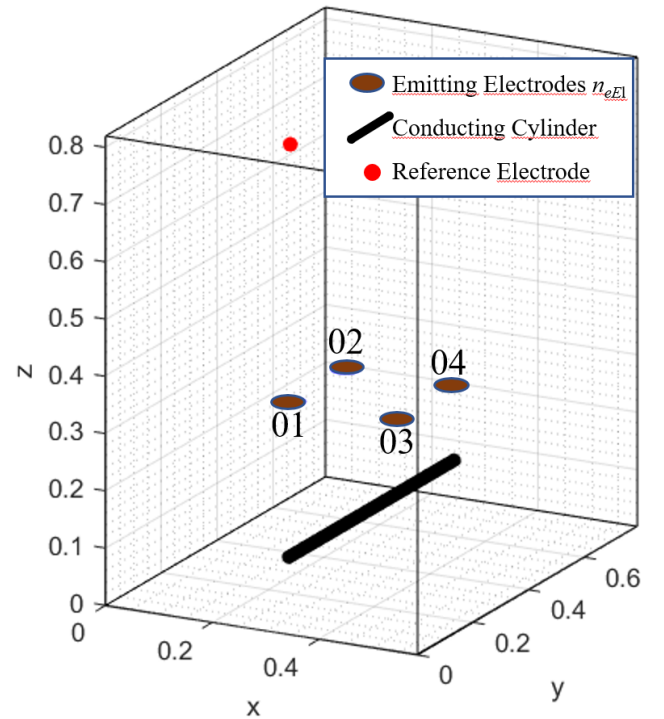


Fig. 3: Modeled underwater environment for simulation of the EIT-array designs.

The environment has the dimension of $x = 0.585$ m, $y = 0.79$ m and $z = 0.82$ m filled with sea water to model a realistic underwater environment. We assume a electrical conductivity of $\sigma_w = 4$ S/m and a relative permittivity of $\epsilon_w = 81$ [15]. The coordinate system's origin for the following positioning is set to the corner of this environment.

Also, a cylinder with metallic conductive properties is integrated into the model of the underwater environment. This object must be detected in the following. The cylinder represents a copper conductor that has an influence on the propagation of the current flow in the water. The dimensions of the conductor are based on a copper rod that has already been used for measurements in our laboratory environment. We defined an electrical conductivity of $\sigma_c = 60 \cdot 10^6$ S/m and relative permittivity of $\epsilon_c = 1$ to realistically represent its electrical properties. The center of the cylinder footprint is

¹<https://git.mylib.th-luebeck.de/sven.ole.schmidt/eit-array-comparison-for-object-detection>

located at $P_{cyl} = (x, z) = (0.2925, 0.1)$ m while it extends for 0.6 m centered in y -direction. The conductor is also depicted in Figure 3.

Note, that for simulation, we will neglect the inhomogeneity of the sea water and the conductor, as well as thermal effects and simulation noise. Under this assumptions, still suitable solutions results, as shown in [11].

For comparability of the designs we will split up the emitting and measuring electrodes in the following to two arrays. We install a plane of four emitting electrodes with index $n_{eEl} = 1, \dots, 4$, while each of the electrodes is a copper disc with a diameter of $d_{eEl} = 5$ cm. By enlarging the electrodes, the transition resistance between electrode and environment is decreased, which leads to lower power losses. The electrodes are arranged in a 2×2 -square with a spacing of 20 cm between the neighbored electrodes. We choose the emitting electrode array's position in the way, that the cylinder is directly below it to optimize the detection setup. The coordinates of the simulated electrode's centers are listed in Table I as well as shown in Figure 3:

TABLE I: Coordinates of the four emitting electrodes in the emitting array

emitting electrode n_{eEl}	position in array [m]
01	(0.1925, 0.295, 0.3)
02	(0.1925, 0.495, 0.3)
03	(0.3925, 0.295, 0.3)
04	(0.3925, 0.495, 0.3)

These electrodes are successively provided in pairs of two with the constant currents $I_1(t) = 1$ A and $I_2(t) = -I_1(t) = -1$ A. This is done for all six electrode combinations, which are labeled by parameter $n_{eC} = 1, \dots, 6$. While the constant current would lead to electrolysis between the electrodes in a real environment, this DC value is chosen, to simplify the statements regarding the detection capability.

In the following, we set the total number of measurement electrodes to twelve with index $n_{mEl} = 1, \dots, 12$ to ensure comparability between designs. Therefore the designs derived in Section III have different numbers of electrodes per plane. The position of the measurement electrodes for all four chosen designs are depicted in Figure 4.

We assume that the diameter of the measurement electrodes is negligibly small. The individual coordinates of the measurement electrodes for all designs are listed in Table II:

As mentioned in Section II, we need to install an additional reference electrode for grounding the measurement electrodes. The reference electrode is placed at $P_{Ref} = (0.1925, 0.295, 0.75)$ in the simulation environment and has the same physical properties as the measurement electrodes. It is also shown in Figure 3.

For all measurement electrode array designs, the emitting electrode array is simulated and the electrical potential is determined twice: First with cylindrical conductor in the environment, subsequently the conductor is removed. So, we manage to focus on the difference between the measurements of the electrical potential. The higher the difference, the higher

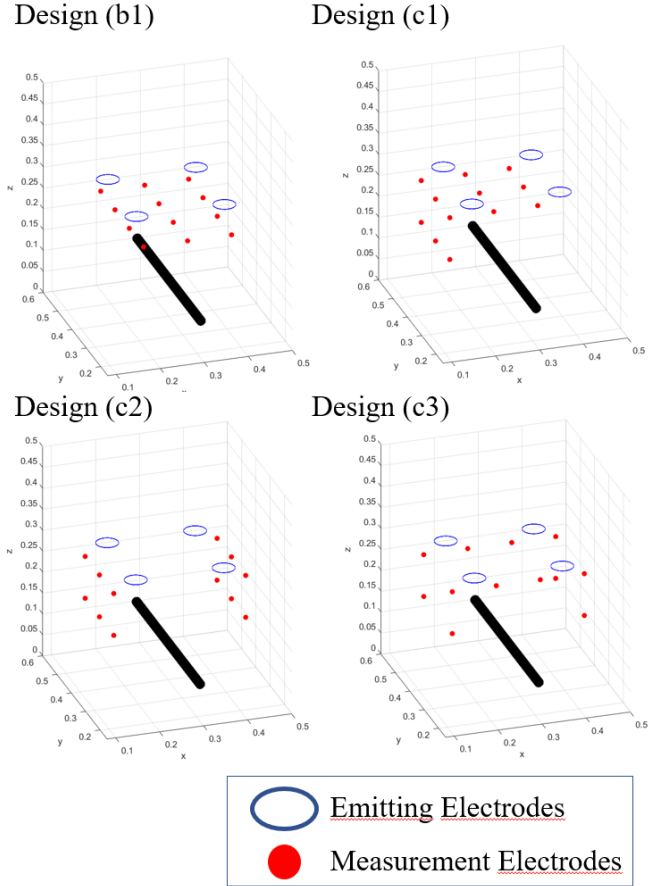


Fig. 4: Position of the twelve measurement electrodes n_{mEl} for the four chosen EIT-array designs.

the influence of the conductor on the potentials and the more likely is the detection of this object based on the potentials.

For detection of objects in an air environment, we compared several distance metrics for target detection systems and found that the ℓ_1 -distance is a good choice [16]. Here, this is adapted for the underwater case. In the following, $U_{n_{mEl}}(n_{eC})$ is the potential perceived by measurement electrode n_{mEl} for emitting electrode combination n_{eC} including the conductor in the environment. And $\hat{U}_{n_{mEl}}(n_{eC})$ is the potential perceived in the same setup, but without including the conductor. Then, each of the designs is characterizable by the ℓ_1 -distance d_{des} with:

$$d_{des} = \sum_{n_{eC}=1}^6 \sum_{n_{mEl}=1}^{12} ||U_{n_{mEl}}(n_{eC})| - |\hat{U}_{n_{mEl}}(n_{eC})||. \quad (1)$$

Note, that both potentials $U_{n_{mEl}}(n_{eC})$ and $\hat{U}_{n_{mEl}}(n_{eC})$ are grounded with respect to the reference electrode's potential. We assume, that the largest ℓ_1 -distance d_{des} leads to the design with the highest detection capability for this evaluation setup.

After introducing the evaluation environment, we will next depict the evaluation results for all four designs.

TABLE II: Coordinates twelve measurement electrodes for the chosen designs sketched in Figure 2. The corresponding Subplots are mentioned next to the Design.

n_{mEl}	design (b1)	design (c1)
01	(0.1925, 0.245, 0.25)	(0.1425, 0.295, 0.175)
02	(0.1925, 0.345, 0.25)	(0.1425, 0.395, 0.175)
03	(0.1925, 0.445, 0.25)	(0.1425, 0.495, 0.175)
04	(0.1925, 0.545, 0.25)	(0.1425, 0.295, 0.275)
05	(0.2925, 0.245, 0.25)	(0.1425, 0.395, 0.275)
06	(0.2925, 0.345, 0.25)	(0.1425, 0.495, 0.275)
07	(0.2925, 0.445, 0.25)	(0.2425, 0.295, 0.275)
08	(0.2925, 0.545, 0.25)	(0.3425, 0.295, 0.275)
09	(0.3925, 0.245, 0.25)	(0.2425, 0.395, 0.275)
10	(0.3925, 0.345, 0.25)	(0.3425, 0.395, 0.275)
11	(0.3925, 0.445, 0.25)	(0.2425, 0.495, 0.275)
12	(0.3925, 0.545, 0.25)	(0.3425, 0.495, 0.275)

n_{mEl}	design (c2)	design (c3)
01	(0.1425, 0.295, 0.175)	(0.1425, 0.295, 0.175)
02	(0.1425, 0.395, 0.175)	(0.1425, 0.495, 0.175)
03	(0.1425, 0.495, 0.175)	(0.1425, 0.295, 0.275)
04	(0.1425, 0.295, 0.275)	(0.1425, 0.495, 0.275)
05	(0.1425, 0.395, 0.275)	(0.4425, 0.295, 0.175)
06	(0.1425, 0.495, 0.275)	(0.4425, 0.495, 0.175)
07	(0.4425, 0.295, 0.175)	(0.4425, 0.295, 0.275)
08	(0.4425, 0.395, 0.175)	(0.4425, 0.495, 0.275)
09	(0.4425, 0.495, 0.175)	(0.2425, 0.295, 0.275)
10	(0.4425, 0.295, 0.275)	(0.3425, 0.295, 0.275)
11	(0.4425, 0.395, 0.275)	(0.2425, 0.495, 0.275)
12	(0.4425, 0.495, 0.275)	(0.3425, 0.495, 0.275)

B. Evaluation of the Simulation Results

After introducing the evaluation setup, we analyze the results of the simulation in this section.

The resulting distances d_{des} for the four chosen designs are shown in Table III:

TABLE III: Distances d_{des} of the designs depicted in Figure 4 for the emitting electrodes $n_{eC,1}$ and $n_{eC,2}$ (The combination is topview-illustrated beneath the indices - Blue: active, White: non active.)

$n_{eC,1/2}$	design (b1)	design (c1)	design (c2)	design (c3)
01 & 02	0.35 mV	0.26 mV	0.18 mV	0.28 mV
01 & 03	0.62 mV	0.66 mV	1.03 mV	0.8 mV
01 & 04	0.49 mV	0.67 mV	1.03 mV	0.79 mV
02 & 03	0.49 mV	0.67 mV	1.04 mV	0.79 mV
02 & 04	0.62 mV	0.67 mV	1.03 mV	0.79 mV
03 & 04	0.35 mV	0.18 mV	0.18 mV	0.28 mV
sum of d_{des}	2.9 mV	3.1 mV	4.5 mV	3.7 mV

Note, that all calculated distances d_{des} of the determined electrical potentials are much greater than the pre-determined variation of the software. Therefore, all four designs are able to detect the existence of a cylindrical conductor based on the change of electric potential.

The 2-dimensional design (b1) covers only the 2-dimensional space. The further an object moves away from the plane of the measurement electrodes, the lower the effect on the induced electrical potentials. We assume, that this will also further decrease the distance d_{des} . In our evaluation, the design achieves a distance sum of 2.9 mV for all combinations $n_{eC,1}$ & $n_{eC,2}$. The difference in electric potential is still

detectable, but this array represents the smallest distance of all evaluated designs.

The 3-dimensional design (c1) consists of two planes, which are perpendicular to each other. Adding a third dimension by rearranging the electrodes increases the distance d_{des} compared to design (b1). Here, the design achieves a distance sum of 3.1 mV.

In design (c2), we arrange the measurement electrodes in two parallel planes. This design promotes the object detection capability. The emitting electrode combinations $n_{eC,1}$ & $n_{eC,2}$, which are also parallel to the planes, have the overall smallest determined distances d_{des} with 0.18 mV each. However, as soon as current flows on a transverse connection between the electrodes, we reach the maximum distance d_{des} of 1.04 mV.

The last evaluated design (c3) includes three planes, which frame the observation area. Similar to design (c2), the combinations $n_{eC,1}$ & $n_{eC,2}$, which run transverse to the parallel side planes, show the strongest distances with 0.8 mV each. For the emitting electrode combinations parallel to the side planes, we get much weaker distances of 0.28 mV.

In general, we find that the ℓ_1 -distance defined in eq. (1) changes for different array designs. The higher this ℓ_1 -distance, the more change of electrical potential between the setup with and without conductor is remarkable. It is recognizable, that the more measurement electrodes are closer to the cylindrical conductor, the higher the ℓ_1 -distance d_{des} and thus the detection capability. Since the conductor will be at an unknown location in a real detection, an arrangement in three dimensions is recommended. In addition, cross-connections leading to transverse current flow wrt. the measurement electrode planes are preferred as combinations, since these had the highest ℓ_1 -distances d_{des} in all four designs.

V. CONCLUSION AND FUTURE WORK

This paper shows the evaluation of 2- and 3-dimensional EIT-arrays for underwater object detection.

After a classification of existence proof of objects, namely *object detection*, in the research field, the basis for the design considerations is laid by the description of EIT. By selectively applying currents to emitting electrodes, EIT causes a current flow through the medium, which is perceived as an induced electric potential by measurement electrodes. The design of the arrays are developed in 1-, 2- and 3-dimensional space. Due to the lack of covering, the 1-dimensional design case and one of the 2-dimensional design concepts will not be pursued further. To ensure comparability of the designs, the array of emitting and measuring electrodes is split. In addition, it is noted that despite the increasing dimension, the number of measurement electrodes remains constant.

Based on these assumptions, four designs were developed and evaluated in a modeled underwater environment. A conductive cylinder is included as the object to be detected, so that the designs are evaluated with and without the cylinder. For the evaluation of the object detection capability of the designs, the ℓ_1 -distance d_{des} was introduced as a metric. This metric sums up the potential differences between the evaluation

setup with and without cylinder for all measurement electrodes. The ℓ_1 -distance changes only by differing the array designs and maximizes at the 3-dimensional designs. Therefore, d_{des} is suitable to mark EIT-arrays, which have a higher chance to detect objects.

Furthermore it is shown, that the current flows through the emitting electrodes parallel to the measurement electrode planes show significantly less ℓ_1 -distance values in the induced potentials. It also follows that a shorter local distance to the detectable object may leads to a higher detection capability.

These results lead to a further development of our EIT array design. It will also be modeled and evaluated using the simulation environment. It is then constructed and tested in a laboratory environment in the aquarium. In parallel, we will adapt our object-detection and localization algorithms. The resulting prototype will be tested for the detection of metallic objects and power cables in water and sediment of a real outdoor scenario.

ACKNOWLEDGMENTS

This publication results from the research of the Center of Excellence CoSA at the Technische Hochschule Lübeck and funded by the Federal Ministry of Economic Affairs and Energy of the Federal Republic of Germany (Id 03SX467B, Project EXTENSE, Project Management Agency: Jülich PTJ). Horst Hellbrück is an adjunct professor at the Institute of Telematics of University of Lübeck.

REFERENCES

- [1] T. Szyrowski, S. K. Sharma, R. Sutton, and G. A. Kennedy, "Developments in subsea power and telecommunication cables detection: Part 1-visual and hydroacoustic tracking," *Underwater Technology*, vol. 31, no. 3, 2013.
- [2] H.-P. Tan, R. Diamant, W. K. Seah, and M. Waldmeyer, "A survey of techniques and challenges in underwater localization," *Ocean Engineering*, vol. 38, no. 14, pp. 1663–1676, 2011. [Online]. Available: <https://www.sciencedirect.com/science/article/pii/S0029801811001624>
- [3] Y. H. Pei and H. G. Yeo, "Uxo survey using vector magnetic gradiometer on autonomous underwater vehicle," in *OCEANS 2009*, 2009, pp. 1–8.
- [4] J. A. Young and D. A. Clark, "Magnetic tensor gradiometry in the marine environment," in *2010 International Conference on Electromagnetics in Advanced Applications*, 2010, pp. 701–704.
- [5] A. Salem, T. Hamada, J. K. Asahina, and K. Ushijima, "Detection of unexploded ordnance (uxo) using marine magnetic gradiometer data," *Exploration Geophysics*, vol. 36, no. 1, pp. 97–103, 2005.
- [6] F. John, R. Kusche, F. Adam, and H. Hellbrück, "Differential ultrasonic detection of small objects for underwater applications," in *Global Oceans 2020: Singapore – U.S. Gulf Coast*, Oct 2020, pp. 1–7, <https://ieeexplore.ieee.org/document/9389186>. [Online]. Available: <http://cosa.th-luebeck.de/download/pub/john-2020-differential-ultrasonic-oceans.pdf>
- [7] X. Bai, M. Hu, T. Gang, and Q. Tian, "An ultrasonic sensor composed of a fiber bragg grating with an air bubble for underwater object detection," *Optics & Laser Technology*, vol. 112, pp. 467–472, 2019. [Online]. Available: <https://www.sciencedirect.com/science/article/pii/S0030399218315184>
- [8] S. A. A. Bakar, N. R. Ong, M. H. A. Aziz, J. B. Alcain, W. M. W. N. Haimi, and Z. Sauli, "Underwater detection by using ultrasonic sensor," *AIP Conference Proceedings*, vol. 1885, no. 1, p. 020305, 2017. [Online]. Available: <https://aip.scitation.org/doi/abs/10.1063/1.5002499>
- [9] F. John, M. Cimdins, and H. Hellbrück, "Underwater ultrasonic multipath diffraction model for short range communication and sensing applications," *IEEE Sensors Journal*, vol. 21, no. 20, pp. 22 934–22 943, 2021.
- [10] G. Bouchette, P. Church, J. E. Mcfee, and A. Adler, "Imaging of compact objects buried in underwater sediments using electrical impedance tomography," *IEEE transactions on geoscience and remote sensing*, vol. 52, no. 2, pp. 1407–1417, 2013.
- [11] A. Schuldei, F. John, G. Ardel, T. Suthau, and H. Hellbrück, "Development of an Electro Impedance Tomography-based Platform for Measurement of burial Depth of Cables in Subsea Sediments," in *Oceans 2019*, 2019.
- [12] F. John, S. O. Schmidt, and H. Hellbrück, "High Precision Open Laboratory 3D PositioningSystem for Automated Underwater Measurements," in *Oceans 2021*, 2021.
- [13] F. John, S. O. Schmidt, and H. Hellbrück, "Flexible arbitrary signal generation and acquisition system for compact underwater measurement systems and data fusion," in *OCEANS 2021 San Diego – Porto*, 2021, pp. 1–6.
- [14] V. Kolehmainen, M. Lassas, and P. Ola, "The inverse conductivity problem with an imperfectly known boundary," *SIAM Journal on Applied Mathematics*, vol. 66, 07 2006.
- [15] N. Nasir, N. Yahya, M. Akhtar, and M. Kashif, "Modeling of antenna for deep target hydrocarbon exploration," *Journal of Electromagnetic Analysis and Applications*, vol. 04, 09 2011.
- [16] M. Cimdins, M. Pelka, and H. Hellbrück, "Sundew: Design and Evaluation of a Model-based Device-free Localization System," in *The Ninth International Conference on Indoor Positioning and Indoor Navigation (IPIN)*, Nantes, France, 2018.